Adsorption of two-dimensional vesicles

1993 J. Phys. A: Math. Gen. 26 1299

(http://iopscience.iop.org/0305-4470/26/6/013)

J. Phys. A: Math. Gen. 26 (1993) 1299–1311. Printed in the UK

Adsorption of two-dimensional vesicles

Damien P Foster and Flavio Seno
Theoretical Physics, 1 Keble Road, Oxford, UK

Received 31 July 1992, in final form 20 November 1992

Abstract. In this paper we discuss the critical behaviour of two-dimensional vesicles with osmotic pressure, but no bending energy, in the presence of an attractive boundary. The phase diagram is presented for the first time and exponents are calculated in the various regions of the phase diagram from an exact enumeration in conjunction with series analysis techniques. In particular special surface critical exponents are presented for the branched polymer phase.

1. Introduction

Membranes often occur in nature as vesicles [1], that is closed surfaces isomorphic to the sphere. A good example of such a surface is the red blood cell [2]. A red blood cell is essentially composed of a membrane formed by a lipid bilayer of amphiphilic molecules. Each of these molecules has a hydrophilic head and one or more hydrophobic tails. In order to avoid contact between the tails and water in the blood, the molecules align themselves into two layers; the tails inside and the heads outside. These layers create a surface, which then closes on itself to form the vesicles.

From a chemical and biological standpoint it is important to know what other substances are contained within the vesicle, but from a physical point of view it is their configurational properties which are of interest. It is well known that under different physical and chemical conditions their average shapes differ widely [1,3,4]. The understanding of these morphologies, and their fluctuations, is an important aspect of the study of vesicles in the field of statistical mechanics.

The most relevant physical parameters in determining the structure of vesicles are expected to be the osmotic pressure difference between the inside and outside [3], and the rigidity of the membrane [5]. The first effect arises because the membrane which forms the vesicles is semi-permeable, and the molecules from the surrounding fluid may diffuse across it via a process of osmosis, which sets up a pressure difference

$$\Delta p = p_{\text{int}} - p_{\text{ext}}. \tag{1}$$

This pressure difference may be positive or negative.

Given the complexity of the behaviour of vesicles in three dimensions [4,6,7], much of the currenf research is on two-dimensional models of closed rings incorporating the parameters discussed. Here there are a number of results, both numerical and analytical.

0305-4470/93/061299+13$07.50

In the absence of rigidity, Monte Carlo studies [8] and, more recently, exact results [9, 10], have shown that two-dimensional vesicles in the bulk show three distinct types of behaviour, depending on the pressure difference:

1. For $\Delta p < 0$ the vesicles are deflated, and appear to have the same critical behaviour as branched polymers.
2. For $\Delta p = 0$ the models reduce to those for a self-avoiding ring, with the associated critical behaviour. The vesicles are then said to be flaccid.
3. For $\Delta p > 0$ the vesicles are inflated, adopting in continuum models a spherical geometry. For models on a lattice they take the configurations with maximal area, the shape of which depends on the lattice. It will be shown later that, in terms of the critical behaviour, this phase is pathological.

While there have been a number of studies of the effect of osmotic pressure in two-dimensional vesicles, few results are available when an attractive surface is included [11, 12]. To date the study of vesicles in the presence of a surface has focused on the shape of the vesicle when the rigidity plays a significant role. Instead in this paper we shall be interested in the critical behaviour of two-dimensional vesicles with an osmotic pressure difference in the presence of an attractive boundary in the limit where the bending energy is negligible and in particular in the determination of critical exponents in different regions of the phase diagram. The vesicle interacts with the surface through a short ranged potential. When this interaction is small the vesicle is unbound, with a vanishing fraction of its perimeter touching the boundary, and displays bulk type behaviour. Above a critical interaction strength the vesicle undergoes a binding transition to a phase where the fraction of the vesicle's perimeter touching the boundary becomes finite.

The remainder of this paper will be structured as follows. In section 2 we introduce the model studied, then in section 3 we discuss the exact enumeration method used to generate the data from which the main results of this paper are derived. In section 4 we present the phase diagram for this model and discuss its features, in section 5 we present results for the critical exponents both at the ordinary and special transitions for different values of the osmotic pressure difference and in section 6 we make some concluding remarks.

2. The model

We model vesicles by polygons on a semi-infinite square lattice. A polygon of perimeter N is simply a closed self-avoiding ring. The osmotic pressure difference between the interior and exterior of the vesicle gives rise to an energy of the form

$$E_p = -\Delta p A \tag{2}$$

where A is the area enclosed. The polygon is allowed to gain an energy, K, for every step on the surface which bounds the semi-infinite plane. This is shown in figure 1.

To study the critical behaviour of this model, we introduce a grand canonical partition function, given by

$$Z = \sum_{\text{rings}} \omega^N \kappa^{N_s} \tau^A \tag{3}$$

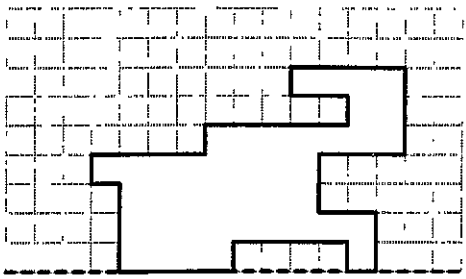

Figure 1. A lattice polygon; the heavy dotted line indicates the surface, while the shaded region shows the enclosed area. Here $N = 46$, $N_S = 5$ and $A = 42$.

where N is the perimeter of the ring, N_S is the number of steps in the surface, ω is the step fugacity, $\kappa = \exp(-K/k_BT)$ and $\tau = \exp(\Delta p/k_BT)$. The sum is carried out over all possible 'unrooted' ring configurations, that is ring configurations which are identical modulo translation, with the constraint that at least one of the steps must lie on the surface. The thermodynamic limit corresponds to N diverging. The average length is controlled by the step fugacity, ω, and the divergence of the length defines a critical value of ω as a function of κ and τ, $\omega_c(\kappa, \tau)$. The average perimeter of the ring, $\langle N \rangle$, and the average number of contacts with the surface, $\langle N_S \rangle$, are given in the usual way by

$$\langle N \rangle = \omega \frac{\partial \log \mathcal{Z}}{\partial \omega} \tag{4}$$

$$\langle N_S \rangle = \kappa \frac{\partial \log \mathcal{Z}}{\partial \kappa}. \tag{5}$$

The canonical partition function for polygons of length N with at least one step on the boundary, $C_N^S(\kappa, \tau)$, is defined by

$$C_N^S(\kappa, \tau) = \sum_{N_S=1}^{N_S^{max}} \sum_{A=A_{min}}^{A_{max}} C_{N,N_S,A}\, \kappa^{N_S} \tau^A \tag{6}$$

where $C_{N,N_S,A}$ is the number of configurations of perimeter N, area A and with N_S contacts with the surface. N_S^{max} is the largest number of contacts with the wall for a polygon of length N, that is $N_S^{max} = (N-2)/2$. A_{min} and A_{max} are the smallest and largest areas for a polygon of length N, and are given by $A_{min} = (N-2)/2$, and $A_{max} = N^2/16$ if $N/2$ is even or $A_{max} = (N^2-4)/16$ otherwise.

The number of unrooted ring configurations of length N on the square lattice without surface or osmotic pressure is known to behave asymptotically as [13]

$$C_N \sim \omega_c^{-N} N^{\alpha-3} \tag{7}$$

defining the bulk exponent α. We expect that $C_N(\kappa, \tau)$ will be governed asymptotically by a similar expression

$$C_N^S(\kappa, \tau) \sim \omega_c(\kappa, \tau)^{-N} N^{\alpha^S-3}. \tag{8}$$

We differentiate between α^S and α, since here the polygons are constrained to have at least one plaquette on the surface, and so α^S is a surface exponent which will in general differ from α. For $\kappa = 1$, $\alpha = \alpha^S$ since the constraint of having one step

in contact with a surface does not change the allowed configurations with respect to the bulk, as the surface simply touches the lowest lying horizontal bond, that is $C_N \equiv C_N^S(1,1)$.

It is convenient to rewrite the partition function explicitly as

$$\mathcal{Z} = \sum_{N=0}^{\infty} C_N^S(\kappa,\tau)\omega^N. \tag{9}$$

It is also of interest to consider the average radius of gyration, defined as the average distance of the sites visited by the perimeter from their common centre of gravity. The thermal average radius of gyration is then given by

$$\langle R_G \rangle = \frac{1}{\mathcal{Z}} \sum_{N=0}^{\infty} \sum_{N_S=1}^{N_S^{max}} \sum_{A=A_{min}}^{A_{max}} R_{N,N_S,A}\ \omega^N \kappa^{N_S} \tau^A \tag{10}$$

where $R_{N,N_S,A}$ is the sum of the radii of gyration for polygons of length N with N_S steps on the surface and area A.

$\mathcal{Z}$ and $\langle R_G \rangle$ diverge as $\omega \to \omega_c$ as follows

$$\mathcal{Z} \sim (\omega_c - \omega)^{2-\alpha^S} \tag{11}$$

$$\langle R_G \rangle \sim (\omega_c - \omega)^{-\nu} \tag{12}$$

where ν is the usual correlation length exponent.

In the bulk it is possible to define a set of rooted polygons, that is rings constrained to pass through a specific point on the lattice. The number of rooted polygons is related to C_N by

$$C_N^{rooted} = N C_N. \tag{13}$$

The situation is slightly different if the rooting point is fixed to a surface; in this case the 'surface rooted' configurations are related to the unrooted configurations with at least one step on the surface through

$$C_{N,N_S,A}^{SR} = N_S C_{N,N_S,A} \tag{14}$$

which, after summing over N_S and A, gives

$$C_N^{SR} = \langle N_S \rangle C_N^S \tag{15}$$

where 'SR' indicates that the rings are 'surface rooted'.

The number of surface contacts scales asymptotically as [14]

$$\langle N_S \rangle \sim N^{\phi_S} \tag{16}$$

where ϕ_S is the surface crossover exponent. In the part of the phase diagram where the vesicle is not adsorbed $\phi_S = 0$ and in the fully adsorbed phase $\phi_S = 1$. In general ϕ_S will adopt a non-trivial value at the adsorption transition. From equations (8), (15) and (16) it is then clear that, for large N

$$C_N^{SR} \sim \omega_c^{-N} N^{\alpha^S + \phi_S - 3}. \tag{17}$$

A new exponent α^{SR} is introduced, defined such that

$$C_N^{SR} \sim \omega_c^{-N} N^{\alpha^{SR} - 3}. \tag{18}$$

3. Exact enumeration of vesicles

In this section the exact enumeration for vesicles on a lattice with pressure and an adsorbing substrate is described. First it is appropriate to discuss briefly some of the previous exact enumeration studies of polygons on a lattice, so the work presented here may be better appreciated in its context. This discussion will be limited to the work on the square lattice.

Guttmann and Enting [15] enumerated polygons up to 56 steps on the square lattice using a novel technique which allowed them to greatly reduce the rate at which the computational effort scales with the size of the rings considered. In this study they only considered the number of such rings, but none of the other quantities of interest in the problem of vesicles. In a later study Enting and Guttmann calculated the number of configurations of polygons of perimeter N and area A up to and including $N = 42$ [16]; later Guttmann added the data for $N = 44$ (unpublished). In order to achieve these values of N they chose not to consider the radius of gyration. Instead they calculated the 'calliper size' in a fixed direction. The calliper size is the linear distance spanned by the polygon in a chosen direction. This is expected to scale in the same way as the radius of gyration.

It was shown by Privman and Rudnick [17] that the radius of gyration gives much better results for the determination of ν. Calculating the radius of gyration for polygons up to $N = 28$ they obtained a value of $\nu = 0.750 \pm 0.0015$ compared with $\nu = 0.753 \pm 0.007$ proposed by Guttman and Enting from calliper sizes for polygons up to $N = 54$ [15]. Privman and Rudnick [17] restricted their attentions to counting the configurations of self-avoiding rings as a function of the perimeter, not considering the area.

In this paper we calculate, for the first time, the coefficients $C_{N,N_s,A}$ and $R_{N,N_s,A}$ defined in equations (9) and (10).

The approach adopted here is to build ring closure into the algorithm from the outset, avoiding the necessity to check for it. This is done by representing the configurations by two vectors, one containing information on the links in the x direction and the other on the y direction. Let these vectors be denoted $\boldsymbol{X}$ and $\boldsymbol{Y}$ respectively. The enumeration proceeds by considering polygons with N_x steps parallel to the x direction, where N_x must be even to allow for ring closure. Both $\boldsymbol{X}$ and $\boldsymbol{Y}$ are initialized with N_x elements. The elements of $\boldsymbol{X}$ correspond, moving anticlockwise around the vesicle, to horizontal steps, taking the value $+1$ if the step is to the right and -1 if the step is to the left. The first element of $\boldsymbol{X}$ is set to $+1$ to avoid double counting. The vector $\boldsymbol{Y}$ contains the vertical height jumped between the horizontal steps. The elements of $\boldsymbol{Y}$ may be positive, negative or zero, with the additional restrictions that the sum of the elements must be zero, and the the sum of the positive elements is half the remaining steps unaccounted for by $\boldsymbol{X}$, that is $(N - N_x)/2$. If these constraints are imposed then all generated configurations are guaranteed to correspond to closed rings. As an example, the polygon shown in figure 2 is described by

$$\boldsymbol{X} = (+1,-1,+1,-1,-1,-1,-1,+1,+1,+1) \tag{19}$$

$$\boldsymbol{Y} = (+1,+1,+1,0,0,0,-2,-1,0,0). \tag{20}$$

The rings are then counted by enumerating, using a binary representation, all possible vectors $\boldsymbol{X}$ with an equal number of $+1$ and -1 elements. For each $\boldsymbol{X}$ all

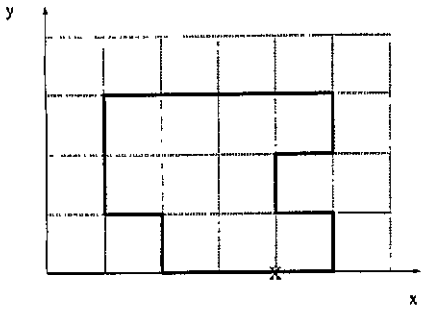

Figure 2. A lattice polygon. X marks the rooting to the boundary.

the consistent vectors Y are calculated. Local self-avoidance is easy to check for, it is simply necessary to ensure that the elements of Y which separate a $+1$ from a -1 are different from 0. Global self-avoidance is more laborious, but essentially consists of checking that the loop does not return to the origin too early, and that no two steps lie on the same bond. The only trick here is to order the checking in such a way that as many similar loops as possible are discarded together. Suitable fine tuning of these checks reduced our CPU usage by more than 50%. Given a particular valid pair of vectors, X and Y, it is easy to calculate N_S, A. The calculation of the coefficients for $N = 32$ required about one week of CPU time on a Sun SPARC station.

Table 1. Table of coefficients for $\tau = 1$, $\kappa = 1$.

N	$C_N^S\langle R_G^2\rangle N^2$	$C_N^S\langle R_x^2\rangle N^2$	C_N^S
4	8	4	1
6	66	33	2
8	600	300	7
10	5164	2582	28
12	42872	21436	124
14	346828	173414	588
16	2754056	1377028	2938
18	21549780	10774890	15268
20	166626744	83313372	81826
22	1275865332	637932666	449572
24	9690096824	4845048412	2521270
26	73090383120	36545191560	14385376
28	548064459968	274032229984	83290424
30	4088719617824	2044359808912	488384528
32	30367415294800	15183707647400	2895432660

While the full table of coefficients is too long to be presented here, tables for $C_N^S(\kappa,\tau)$ and $R_N(\kappa,\tau)$ are given for $\tau = 0$ and 1 at $\kappa = 1$ and $\kappa = \kappa_c$ in tables 1–4†. These tables give the series from which the results for the pure branched polymer and self-avoiding ring limits, presented in section 4, are calculated. Results for $\tau = 1$ are given in table 1, extending the results of Privman and Rudnick to $N = 32$ [17].

In tables 1 and 3 the coefficients $C_N\langle R_G\rangle N^2$, $C_N\langle R_x\rangle N^2$ and C_N are tabulated because they have integer values when $\tau = \kappa = 1$. In tables 2 and 4 slightly different coefficients are presented, since C_N vanishes for $\tau = 0$. The appropriate modification is to substitute C_N by $C_{N/2-1}^{BP}$, the number of branched polymer configurations of

† The full table of coefficients is available on floppy disk by request.

Table 2. Table of coefficients for $\tau = 0$, $\kappa = 1$.

N	$C^{BP}_{N/2-1}\langle R_G^2\rangle N^2$	$C^{BP}_{N/2-1}\langle R_x^2\rangle N^2$	$C^{BP}_{N/2-1}$
4	8	4	1
6	66	33	2
8	504	252	6
10	3170	1585	18
12	17720	8860	55
14	93214	46607	174
16	469968	234984	566
18	2282892	1141446	1868
20	10770040	5385020	6237
22	49679322	24839661	21050
24	224921256	112460628	71666
26	1002256080	501128040	245696
28	4406005560	2203002780	847317
30	19145185020	9572592510	2937116
32	82351698016	41175849008	10226574

Table 3. Table of coefficients for $\tau = 1$, $\kappa = 2.05$.

N	$C^{S}_{N}\langle R_G^2\rangle N^2$	$C^{S}_{N}\langle R_x^2\rangle N^2$	C^{S}_{N}
4	16.400000	8.200000	2.050000
6	206.332500	87.022500	6.252500
8	2402.682000	991.257000	27.372625
10	25109.359656	10139.695906	131.774256
12	242875.428642	97070.318699	672.845375
14	2231030.034529	886724.941119	3598.469871
16	19754963.654335	7826463.043522	19946.151073
18	170048569.275293	67230505.279980	113565.047274
20	1431244025.252075	565097587.963967	660291.931617
22	11828976194.066471	4666284579.613015	3904886.687046
24	96304444458.703522	37967395387.500854	23419889.500127
26	774203298243.066895	305100796403.966553	142131854.799101
28	6157246268504.137695	2425804140719.424805	871307287.005438
30	48516247299385.039062	19110719306407.285156	5387968162.548672
32	379209199701545.000000	149354179954834.250000	33571343916.596840

$N/2 - 1$ steps, corresponding to vesicle configurations of minimal area. The step fugacity calculated from this series is not ω, but the step fugacity for the branched polymer, $\omega^2\tau$. As all the coefficients C_N are zero, $\omega \to \infty$, but the product $\omega^2\tau$ is finite, and so the problem is still well behaved.

4. The phase diagram

In this section the phase diagram in the κ–τ plane is discussed, along with the method of its determination. The phase diagram is shown in figure 3.

As the model studied demands that at least one step lie on the boundary, it is clear that when the vesicle is inflated, there will be a finite number of monomers in contact with the surface for all values of κ; it is therefore not sensible to discuss the surface behaviour for $\tau > 1$. For the remainder of this section we shall concentrate on the region $\tau \leqslant 1$.

Table 4. Table of coefficients for $\tau = 0$, $\kappa = 2.25$.

N	$C^{BP}_{N/2-1}\langle R_G^2\rangle N^2$	$C^{BP}_{N/2-1}\langle R_x^2\rangle N^2$	$C^{BP}_{N/2-1}$
4	18.000000	9.000000	2.250000
6	241.312500	99.562500	7.312500
8	2450.250000	932.625000	28.265625
10	19023.925781	6704.472656	102.550781
12	126155.039062	41944.394531	364.086914
14	769813.200439	245713.519775	1316.559814
16	4401818.200195	1361919.520020	4792.830139
18	23814729.411575	7181962.208267	17398.580521
20	123693937.005157	36522611.612320	63278.341953
22	622332445.970189	180529387.438165	230801.723027
24	3047534829.350086	870818668.657625	842818.749478
26	14587479138.287060	4114205441.927525	3080342.005214
28	68501542315.455917	19099517477.059547	11269790.752239
30	316425477700.582520	87334308428.331284	41269435.711970
32	1440815604974.533936	394088984528.986816	151239687.901549

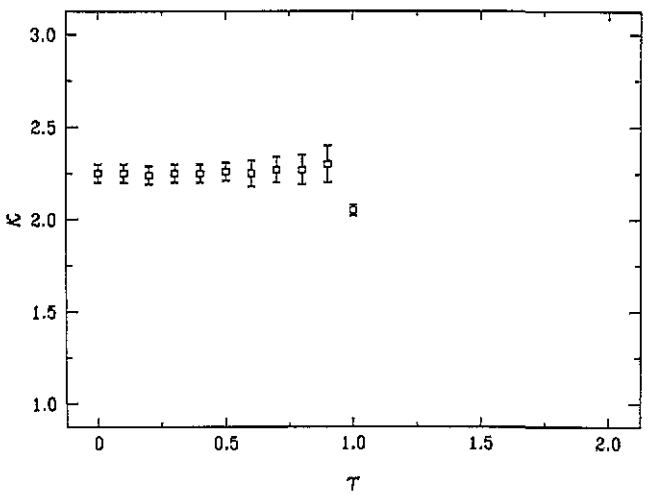

Figure 3. The phase diagram in the κ, τ plane. The full curve corresponds to the transition between the bound and unbound phases. X indicates the location of the adsorption transition for $\tau = 1$. The dotted and broken curves correspond to lines of first-order transitions separating the bound and unbound phases, respectively, from the inflated phase.

The difficulty in determining the phase diagram is the systematic identification of the critical value of the surface interaction, $\kappa_c(\tau)$. It is known that ω_c is a constant as a function of κ up to and including $\kappa_c(\tau)$ [14]. This has been used to good effect as a method for determining the adsorption transition in a number of related problems, such as the adsorption of self-avoiding walks [18,19] and branched polymers [20,21], where the adsorption transition is identified as the point at which ω_c begins to drop as κ is increased. This procedure forms the basis of the method adopted here. The main difficulty with this method is the accurate determination of ω_c from the finite series of coefficients. The methods adopted here include the method of differential approximants [22,23], Padé analysis [24] and the Guttmann–Joyce recurrence method [25]. While the methods gave consistent results, the method of differential approximants was found to be more stable.

Figure 4 shows ω_c plotted as a function of κ for $\tau = 1$ calculated using the method of differential approximants. It is expected that the transition will be at the same point as for the self-avoiding walk, found by Guim and Burkhardt to be

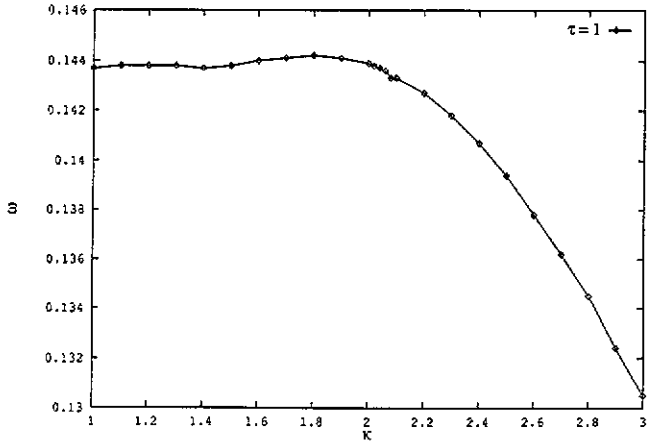

Figure 4. Plot of ω_c against κ for $\tau = 1$.

$\kappa = 2.044 \pm 0.002$ [26]. The location of the transition is found by determining where ω_c begins to fall significantly as a function of κ. Figure 4 is representative of the values given by the table of approximants. To correctly determine the errors associated with the localization of the transition it is necessary to consider also the spread of values given in the table of approximants. It is found that ω_c begins to drop at a value of $\kappa = 2.05 \pm 0.03$, indicating that the transition occurs in the same place, within numerical errors.

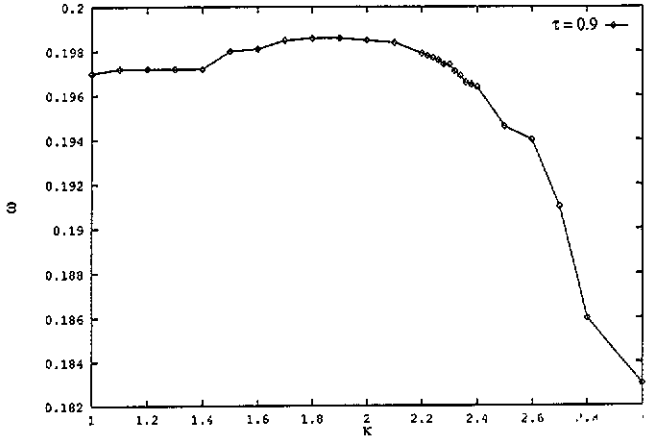

Figure 5. Plot of ω_c against κ for $\tau = 0.9$.

Numerically it is observed that the value of κ required for adsorption decreases slowly as τ is decreased for $\tau < 1$. While the series analysis results are quite stable at $\tau = 1$, they are very unsteady just below one. Figure 5 shows the plot of ω_c for $\tau = 0.9$. The quality of the plot is not as good as that in figure 4 because of the difficulty in assigning a single value to each point due to the instability of the table of differential approximants. The lack of precision in the evaluation of ω_c can be understood in terms of finite size effects. With a finite number of coefficients we might expect a strong influence of the self-avoiding ring fixed point implying that as $\tau \to 1$, the stronger the influence of the adsorption fixed point at $\tau = 1$ on the results becomes, giving a loss of accuracy, reflected in the increase of the error bars

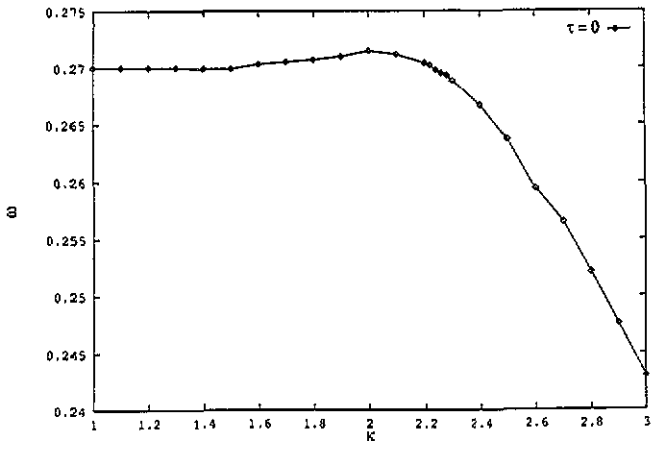

Figure 6. Plot of ω_c^{BP} against κ for $\tau = 0$, where $\omega^{BP} = \omega^2\tau$.

shown in figure 3. It is probable that the true phase boundary display a slight drop as a function of τ and then fall sharply between $\kappa = 0.9$ and 1.0 giving a continuous line upto and including $\tau = 1$. The series obtained here is insufficient to verify this. Figure 6 shows the plot of ω_c^{BP} for $\tau = 0$, where $\omega^{BP} = \omega^2\tau$. The transition occurs at $\kappa = 2.25 \pm 0.05$. These are consistent with results published recently by Lookman *et al* [21] who looked directly at the problem of the adsorption of a lattice tree to a surface using an identical method.

5. The critical exponents

Having determined the general shape of the phase diagram, it is now of interest to calculate the exponents defined in section 2 and determine how they vary in the different parts of the phase diagram.

Setting $\kappa = 1$ and $\tau = 1$, where the polygon behaves like a self-avoiding ring, and using the method of differential approximants, the exponents are found to be

$$\alpha^S = 0.50 \pm 0.03 \tag{21}$$

$$\alpha^{SR} = 0.50 \pm 0.04 \tag{22}$$

$$\nu = 0.750 \pm 0.005 \tag{23}$$

in good agreement with previous results [27] and satisfy, to within numerical errors, the expected scaling relation $\alpha = 2 - 2\nu$ [14].

As τ was reduced it was found that these exponents changed abruptly. In particular, when $\tau = 0.9$, we found

$$\alpha^S = 2.0 \pm 0.2 \tag{24}$$

$$\alpha^{SR} = 2.0 \pm 0.2 \tag{25}$$

$$\nu = 0.62 \pm 0.04. \tag{26}$$

While these exponents are not as precise as those at $\tau = 1$, they do indicate a change in critical behaviour. This is particularly evident comparing α^S at the two points. It

is believed that for $\tau < 1$ the critical behaviour should be dominated by a branched polymer fixed point [3]. This is consistent with our findings here. For the branched polymer $\nu = 0.64\ldots$ [28,29], which compares well with our result. Additionally, in studies of branched polymers an exponent θ is introduced [29], through

$$C_N \sim \omega_c^{-N} N^{-\theta} \tag{27}$$

which when compared with equation (11) gives

$$\theta = 3 - \alpha^S. \tag{28}$$

Our results imply that $\theta = 1$, which agrees with a known result for the branched polymer [29]. Strictly the θ exponent defined here is a surface exponent which coincides with the usual definition of the bulk exponent when $\kappa = 1$, it would therefore be appropriate to use θ^S to denote, in consistent manner, this fact.

Comparing equations (16), (17) and (27) we obtain the relationship

$$\theta^{SR} = \theta^S - \phi_S \tag{29}$$

using notation consistent with that introduced section 2. In a recent paper De'Bell *et al* [20] derived the relation

$$\theta_1 = \theta + 1 \tag{30}$$

where θ_1 was defined such that $\theta_1 = \theta^{SR} + 1$. This result is only valid in the ordinary regime where $\theta = \theta^S$ and $\phi_S = 0$. Equation (29) provides the correct generalization of this equation to general κ. In terms of the α exponents this equation becomes

$$\alpha^{SR} = \alpha^S + \phi_S. \tag{31}$$

The agreement between our results and those known for the branched polymer improves rapidly as τ decreases from one and the influence of the self-avoiding regime becomes less relevant. In particular when $\tau = 0$ we find

$$\alpha^S = 1.99 \pm 0.02 \tag{32}$$

$$\alpha^{SR} = 2.0 \pm 0.05 \tag{33}$$

$$\nu = 0.645 \pm 0.007. \tag{34}$$

Having verified that our model agrees with previous results for $\kappa = 1$, it is now interesting to investigate the special surface exponents, that is the values of α^S and α^{SR} at the adsorption transition. Because of the uncertainty in the determination of the location of the transition, the exponents could not be determined as accurately as at $\kappa = 1$. The errors are calculated by looking at the values of the exponents at the best and worst estimates of κ_c. For $\tau = 1$ and $\kappa = 2.05$ we find

$$\alpha^S = 1.3 \pm 0.1 \tag{35}$$

$$\alpha^{SR} = 1.8 \pm 0.2 \tag{36}$$

$$\phi_S = 0.51 \pm 0.04. \tag{37}$$

For $\tau = 0$ and $\kappa = 2.25$

$$\alpha^{S} = 2.80 \pm 0.08 \tag{38}$$

$$\alpha^{SR} = 3.45 \pm 0.08 \tag{39}$$

$$\phi_S = 0.6 \pm 0.1. \tag{40}$$

To the best of our knowledge these are the first reported values for exponents at the binding transition of a branched polymer phase (for $d \geqslant 3$ see [7,30]). The exponents α^{S} and α^{SR} calculated at the adsorption transition for the self-avoiding ring are also new and satisfy, to within numerical errors, the scaling relation $\alpha^{S} = 2 - \nu$ [14] expected to hold for self-avoiding rings. In this case ϕ_S agrees with the known exact value, $\phi_S = 0.5$, for the self-avoiding walk [31].

The results at $\tau = 0.9$ were very imprecise, due to both the increased inaccuracy in the determination of the phase boundary, and to instabilities in the series analysis techniques. It was found, however, that $\alpha^{S} = 2.8 \pm 0.5$ and $\alpha^{SR} = 3.4 \pm 0.5$, implying that $\phi_S = 0.6$. These results are consistent with those found at $\tau = 0$.

6. Conclusions and discussion

In this paper we have studied the behaviour of a vesicle in the presence of a surface. When there is no interaction with the surface, our results support the picture presented in the literature, where a transition to branched polymer behaviour is expected when the pressure inside the vesicle becomes less than the pressure outside.

Surface exponents, α^{S} and α^{SR}, were introduced and their values were calculated both in the ordinary and, for the first time, the special regimes. They are expected to coincide with the bulk exponent α when there is no interaction with the surface, but take on new values at the special surface transition.

In equation (29) we have also presented a general relation between different surface exponents. This result correctly extends a relation recently presented by De'Bell *et al* [20].

The numerical results presented in this paper were derived by performing an exact enumeration of all polygon configurations on the square lattice up to 32 steps, keeping track of the enclosed area and number of surface contacts. We extended the existing series for the radius of gyration for polygons in the bulk, presented by Privman and Rudnick [17], by two terms.

A possible extension of the model presented here would be the introduction of a fugacity associated with the number of corners of the polygon in order to study the effect of rigidity on the adsorption behaviour.

Acknowledgments

We would like to thank Carlo Vanderzande for helpful discussions. DPF would like to acknowledge support from the SERC and FS would like to acknowledge support from the EC through the SCIENCE programme.

References

[1] Leibler S, Singh R R P and Fisher M E 1987 *Phys. Rev. Lett.* **59** 1989
[2] Leibler S 1989 *Statistical Mechanics of Membranes and Surfaces* ed D R Nelson, T Piran and S Weinberg (Singapore: World Scientific)
[3] Fisher M E 1989 *Physica* **38D** 112
[4] Lipowski R 1991 *Nature* **349** 475
[5] Canham P B 1970 *J. Theor. Biol.* **26** 61
[6] Orlandini E and Tesi M C 1992 *Physica* **185A** 160
[7] Orlandini E, Stella A L, Sullivan F and Tesi M C 1992 *Preprint*
[8] Maggs A C, Leibler S, Fisher M E and Camacho C J 1990 *Phys. Rev.* A **42** 691
[9] Fisher M E, Guttmann A J and Whittington S 1991 *J. Phys. A: Math. Gen.* **24** 3095
[10] Banavar J R, Maritan A and Stella A L 1991 *Phys. Rev.* A **43** 5752
[11] Maggs A C and Leibler S 1990 *Europhys. Lett.* **12** 19
[12] Seifert U 1991 *Phys. Rev.* A **43** 6803
[13] Hammersley J M and Welsh D J A 1962 *Quart. J. Math.* **13** 108
[14] Binder K 1983 *Phase Transitions and Critical Phenomena* vol 8, ed C Domb and J L Lebowitz (New York: Academic)
[15] Guttmann A J and Enting I G 1988 *J. Phys. A: Math. Gen.* **21** L165
[16] Enting I G and Guttmann A J 1990 *J. Stat. Phys.* **58** 475
[17] Privman V and Rudnick J 1985 *J. Phys. A: Math. Gen.* **18** L789
[18] De'Bell K and Essam J W 1980 *J. Phys. C: Solid State Phys.* **13** 4811
[19] Foster D P, Orlandini E and Tesi M C 1992 *J. Phys. A: Math. Gen.* **25** L1211
[20] De'Bell K, Lookman T and Zhao D 1991 *Phys. Rev.* A **44** 1390
[21] Lookman T, Zhao D and De'Bell K 1991 *Phys. Rev.* A **44** 4814
[22] Hunter D L and Baker G A 1979 *Phys. Rev.* B **19** 3808
[23] Guttmann A J 1989 *Phase Transitions and Critical Phenomena* vol 13, ed C Domb and J L Lebowitz (New York: Academic)
[24] Hunter D L and Baker G A 1973 *Phys. Rev.* B **7** 3346
[25] Guttmann A J and Joyce G S 1972 *J. Phys. A: Math. Gen.* **5** L81
[26] Guim I and Burkhardt T W 1989 *J. Phys. A: Math. Gen.* **22** 1131
[27] des Cloizeaux J and Jannink G 1989 *Polymers in Solution: Their Modelling and Structure* (Oxford: Oxford University Press)
[28] Daoud M and Joanny J F 1981 *J. Physique* **42** 1359
[29] Parisi G and Sourlas N 1981 *Phys. Rev. Lett.* **46** 871
[30] Janssen H K and Lyssy A 1992 *J. Phys. A: Math. Gen.* **25** L679
[31] Burkhardt T W, Eisenrigler E and Guim I 1989 *Nucl. Phys.* **316** 559